IRRIGATION WATER PUMPING (IWP) SYSTEMS - COMPARISON BETWEEN PHOTOVOLTAICS AND CONVENTIONAL ENERGY SOURCES

CRPNI SUSTAVI ZA NAVODNJAVANJE (CSN) - USPOREDBA IZMEĐU FOTONAPONSKIH I KONVENCIONALNIH IZVORA ENERGIJE

Mohamed EL-Shimy [1*], Mohamed Nour Eldeen [2], Taha Abdo Mohamed [3]
[1] *Ain Shams University, Electrical power and machines department, Cairo, Egypt*
[2] *Ain Shams University, Irrigation engineering department, Cairo, Egypt*
[3] *SunInfinite Co, Cairo, Egypt*
*E-mail adresa osobe za kontakt / e-mail of corresponding author: mohamed_bekhet@eng.asu.edu.eg

Sažetak: *U radu je prikazana detaljna tehno-ekonomska analiza te analiza emisija stakleničkih plinova (SP) konvencionalnih i solarnih (FN) energetskih izvora energije za crpne sustave za navodnjavanje (CSN). Ključni čimbenici koji utječu na ekonomske karakteristike solarne fotonaponske izvore energije uključuju dimenzije, postupke za usmjeravanje sustava za praćenje kretanja Sunca, te karakteristike proizvodnje (osobito učinkovitosti) solarne-FN tehnologije. Stoga, ovaj rad opisuje dimenzioniranje i optimizaciju praćenja smjera kretanja Sunca za CSN s obzirom na utjecaj različitih FN tehnologija na natapni i "kap po kap" sustav za navodnjavanje. Ekonomske katakteristike i emisije solarnih PV izvora također su prikazani u usporedbi sa konvencionalnim sustavima s obzirom na stvarne troškove proizvodnje energije. Prikazani su poboljšani modeli za proizvodnju energije, dimenzioniranje, određivanje ekonomskih karakteristika i emisija SP. Prikazani CSN, smješten na lokaciji New Kalbsha u regiji Lake Nasser na jugu Egipta, razmatran je kao primjer za uspoređivanje solarnih FN i konvencionalnih izvora energije za CSN. Rezultati pokazuju visoku održivost izvora solarne FN energije za CSN u usporedbi sa distribucijskom električnom mrežom i varijantom sa dizel motorom.*
Ključne riječi: *crpljenje vode za navodnjavanje, solarni fotonaponski sustavi, dizel motori, električna mreža, analiza održivosti.*

Abstract: *This paper presents a detailed techno-economic and greenhouse gasses (GHG) emissions analysis of conventional and solar-PV energy sources for supplying irrigation water pumping (IWP) systems. The key factors affecting the economics of solar-PV energy sources include the size, the sun tracking algorithm, and the energy production characteristics (especially the efficiency) of the solar-PV technologies. Therefore, this paper presents sizing and sun tracking optimization of solar-PV generator for IWP systems considering the impact of various solar-PV technologies for the flood and drip irrigation systems. The economics and emissions of solar-PV sources in comparison with conventional systems are also presented considering the true costs of energy production. Improved models for energy production, sizing, economics and GHG emissions quantification are presented. A proposed IWP project located at the New Kalbsha site near the Lake Nasser region in the south of Egypt is considered as a numerical example for the comparative analysis of solar-PV and conventional energy sources for IWP. The results show the high viability of solar-PV sources for IWP in comparison with the utility grid electricity and diesel engine energy alternatives.*
Keywords: *irrigation water pumping, solar photovoltaics, diesel engines, electricity grid, viability analysis.*

Received: 08.10.2016 / Accepted: 29.11.2016
Published online: 14.12.2016

Znanstveni rad / Scientific paper

1. INTRODUCTION

Conventionally either diesel engines or motor-pump set supplied from the grid electricity are used for Irrigation Water Pumping (IWP); however, the use of these energy sources faces some problems. These problems are associated with the environmental impact, energy supply feasibility, and energy source availability. Generally, both diesel engines and grid electricity are based on fossil fuels. Therefore, they have negative ecological impacts and highly affected by the variable costs of these fuels. With respect to the grid access, it is not economically feasible and technically reliable to extent the electricity grid for covering the energy demand required for irrigation in remote locations. This is due to the low energy and intermittent demand of these types of electrical loads. In addition, supplying these remote locations by diesel fuels may be faced by high transportation costs and risks of fuel unavailability. The problems associated with conventional energy sources open the path to the utilization of renewable energy sources in many applications including IWP. Due to its natural availability, static technologies, and competitive economics, solar photovoltaics (solar-PV) are the most attractive energy alternative in the field of IWP (Lal et al. 2013; Qoaider et al. 2010). Solar-PV systems can also be constructed in any scale starting from micro-scale to large-scale (EL-Shimy et al. 2016; EL-Shimy 2013; Hamidat et al. 2003; Ghoneim 2006). This makes the possibility to perfectly adapt the design of the solar-PV generators to the scale of the considered load.

Since irrigation loads are considered deferrable (i.e. loads that can be shifted in time), the natural variability

and intermittency of the solar energy source do not create a technical challenge (EL-Shimy et al. 2016; EL-Shimy 2013; EL-Shimy May 2015). In addition, neither electrical nor electrochemical energy storage is generally required in IWP applications; however, water storage tanks may be needed in some IWP applications based on the characteristics of the irrigation loads (EL-Shimy et al. 2016; EL-Shimy Nov 2015).

From an economic point of view, solar-PV generating systems have high initial costs but their operation and maintenance (O&M) costs are generally very low in comparison with their conventional counterparts as well as other renewable energy sources (El-Shimy 2012; EL-Shimy 2009; Said et al. 2015; Cloutier 2011). The proper sizing and sun tracking algorithm of solar-PV generators also play a key factor in the economics and the LCOE of these systems. Therefore, this paper presents a systematic method for sizing and sun tracking optimization of solar-PV energy systems. It popular to declare that the Levelized Cost of Energy (LCOE) of solar-PV systems is generally high in comparison with the retail prices of the grid electricity or most of the other conventional counterparts. These economical characteristics are based only on the consideration of the direct costs of energy sources; however, energy sources can be characterized by direct and indirect (or external) costs (Burtraw 2012; Sundqvist 2002).

The true costs of energy include the direct and indirect costs. The indirect costs include the costs associated with health and environmental damages caused by emitting pollutions. The factors that affect the value of the true costs include the population density near a power plant, emitted pollutions, and sustainability. In this paper, the impact of considering the true costs of energy on the economic feasibility and the LCOE of conventional and solar-PV energy alternatives for supplying IWP are investigated. The presented sizing optimization method is based on (EL-Shimy 2013); however, the impacts of various sun tracking options and various available solar-PV technologies on the sizing and economics are considered in this paper. References (Said et al. 2015; EL-Shimy et al. 2016) presented a detailed overview of various solar-PV technologies and sun tracking options as well as their costs. These data is used as input data in this paper. This paper considered also two of the most utilized irrigation approaches. These are the flood and drip irrigation systems. Energy production, economic, and emissions models are presented. The techno-economic and emissions analysis of a proposed large scale irrigation water pumping project is presented as a numerical example. This project is located at the New Kalbsha site near the Lake Nasser region in the south of Egypt. The meteorological conditions and the proposed hydraulic energy demand are available in (EL-Shimy 2013).

2. SOLAR-PV IWP SYSTEM CONFIGURATION AND ENERGY FLOW MODELING

Normally, a solar-PV water pumping system consists of three main components: the solar-PV generator, motor and the pump. Each component has its own operating characteristics, which are the I-V characteristics of the PV array, the power consumption-discharge characteristics of the pump and the torque-speed characteristics of the motor and pump as well. The motor drives the pump whose torque requirements vary with the speed at which it is driven. The motor is operated by the generated power from the solar-PV array whose I–V characteristics depend nonlinearly on the solar irradiance variations and on the temperature of the solar-PV cells and also on the current drawn by the motor (Ghoneim 2006). The solar-PV generator consists of an array of solar-PV modules connected in series–parallel combinations to provide the desired DC voltage and current (Hamidat 2008).

A schematic diagram of the system configuration chosen for the present study is presented in **Fig. 1**. The main system components are: solar-PV array, maximum power point tracker (MPPT), power conditioning device (P.C.D), motor, and pump. The MPPT is adopted here to force the solar-PV array to work at its maximum power, thus improving the system efficiency.

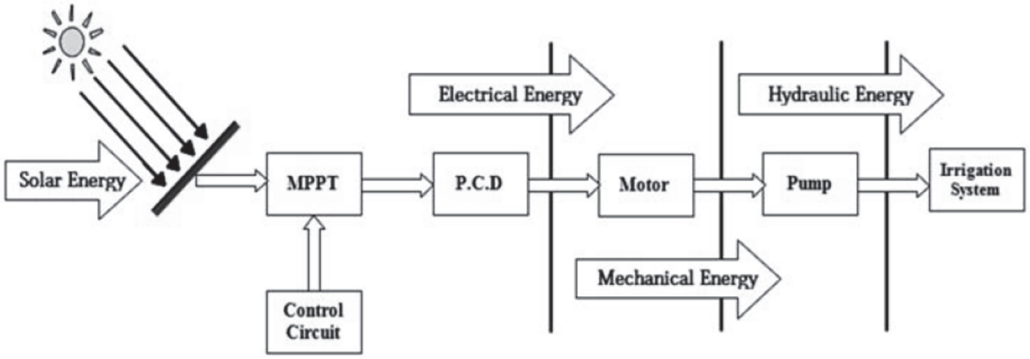

Figure 1. A schematic diagram of the considered solar-PV pumping system for IWT

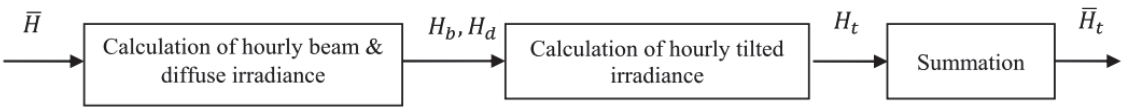

Figure. 2. Model of the solar energy incident on the solar-PV plane

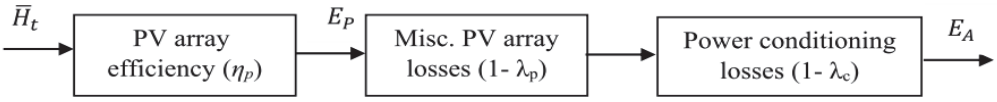

Figure 3. Solar-array energy production model

Two types of pumps are used in the solar-PV pumping systems: (i) centrifugal pumps which are the most common pumps used in the solar-PV pumping applications and (ii) volumetric pumps. The power conditioning device (P.C.D) has a role to optimize the transfer of the energy between the solar-PV array and the motor-pump set. Power conditioning can be a DC/AC inverter for an AC electric motor or a DC/DC converter for a DC electric motor (Hamidat 2008). It is clear from **Fig. 1** that there are four main energies flowing in the solar-PV pumping system starting from the solar energy that received on the surface of the solar-PV modules which is converted instantaneously into electric energy by the solar-PV effect, then the motor that is responsible for the electrical energy conversion into mechanical energy and finally the pump that is responsible for the mechanical energy conversion into hydraulic energy needed for the operation of the specified irrigation system. All the components of the solar-PV pumping system are modeled independently and integrated together for the purpose of performance and sizing optimization.

Solar irradiance on a generally titled plane of the solar-PV array is computed using the following algorithm shown in **Fig. 2**. Details of the mathematical modeling of various blocks in **Fig. 2** are available in (EL-Shimy 2013). The flowchart can be described as a series of three basic steps: The total daily irradiance in the plane of the solar-PV array $\bar{H}_t$ equals the summation of the hourly irradiance in the plane of the solar-PV array H_t, that is $\bar{H}_t = \sum H_t$. The estimation of H_t involves the determination of the hourly beam H_b (or direct) and diffuse H_d irradiance on a horizontal surface for all hours of an average day (i.e. having the same daily global irradiance as the monthly average global irradiance). The monthly average value of daily global irradiance is simply obtained by taking the arithmetic mean of daily values by dividing the monthly global irradiance value (sum of daily values) by the number of days in the corresponding month (EL-Shimy 2013; Duffie et al. 2013; RETScreen 2004; NASA 2016).

A solar-PV cell is a nonlinear power source, the output current and voltage depend on the irradiance level and temperature. Any change in the weather conditions results in a change in the operating point of the solar-PV cell. The solar-PV array model can be represented through the following flowchart shown in **Fig. 3**. The equations describing the energy production model of **Fig. 3** are available in (RETScreen 2004).

The electrical energy generated from the solar-PV has major problems such as the energy conversion efficiency is low, especially under low irradiance conditions, and the amount of generated electric power changes continuously with weather conditions. Thus it becomes necessary to use techniques to extract the maximum power, to achieve maximum efficiency in operation. Connecting a solar-PV module directly to the load enables extraction of 31% energy, which increases to 97% through the use of MPPT. The maximum power extracted from solar-PV cells depends not only on the solar irradiance strength but also on the operating point of the energy conversion system (Faranda et al. 2008).

In general, there is a unique point on the I-V or P-V curve, called the Maximum Power Point (MPP), at which the entire solar-PV system operates with maximum efficiency and produces its maximum output power as shown in **Fig. 4**; this point varies according to the climatic conditions (EL-Shimy Nov 2015; De Brito et al. 2011; Faranda et al. 2008). **Fig. 4** clearly shows that the short circuit current and the MPP are proportional to the solar irradiance. The changes in the solar irradiance have a minor impact on the open circuit voltage. On the other hand, the changes in the cell temperature cause inverse changes in the open circuit voltage and the MPP while their impacts on the short-circuit current are minor. This is due to the inverse relation between the temperature and the efficiency of the solar-PV cells.

The supply of an AC motor by a solar generator in a solar-PV water pumping system requires the use of an inverter which can transform the DC voltage produced by the solar-PV into an AC source. In principle, there are two main types of DC/AC inverters: the self-commutated and the forced-commutated inverter (Duzat et al. 2000; Daud et al. 2005). Generally, the efficiency of the inverter η_i indicates the fraction of the input DC power P_{DC} that is transferred to the output AC side P_{AC}. The inverter efficiency ranges from 95-98% and is defined as the ratio between its output AC power P_{AC} to its input power P_{DC} i.e. $\eta_i = P_{AC}/P_{DC}$. Although there are several alternative motor technologies for the use in IWP (Gopal 2013), the squirrel cage induction motors are considered the perfect choice for modern IWP systems. This is due to the rigidity, low maintenance requirements, long lifetime and low cost of these motors in comparison with other alternatives. The efficiency of an induction motors related to the mechanical power (P_{mech}) furnished to the load and given by $\eta_m = P_{mech}/P_{AC}$. The full load efficiency of induction motors varies from about 85-97 %.

Water pump market offers a variety of configurations, each of which has its fields of applications and features and it may be subdivided into three main types according to their applications: submersible, surface, and floating water pumps. There are another classification of pumps according to their principle of operation such as centrifugal pumps, screw pumps, and piston pumps (RETScreen 2004; Ramos et al. 2009). The selection of an appropriate pump in a solar-PV water pumping application is solely site dependent factors such as water requirement, water height, and water quality (EL-Shimy 2013; RETScreen 2004). The head versus flow rate (Q) usually characterizes the different types of pumps. The 'head' is a term refers to the height of a vertical column of water. The total dynamic

head (H_T) of a pump (or total pumping head) is the sum of the total static head, the pressure head, the friction head, and the velocity head (Bachus et al. 2003).

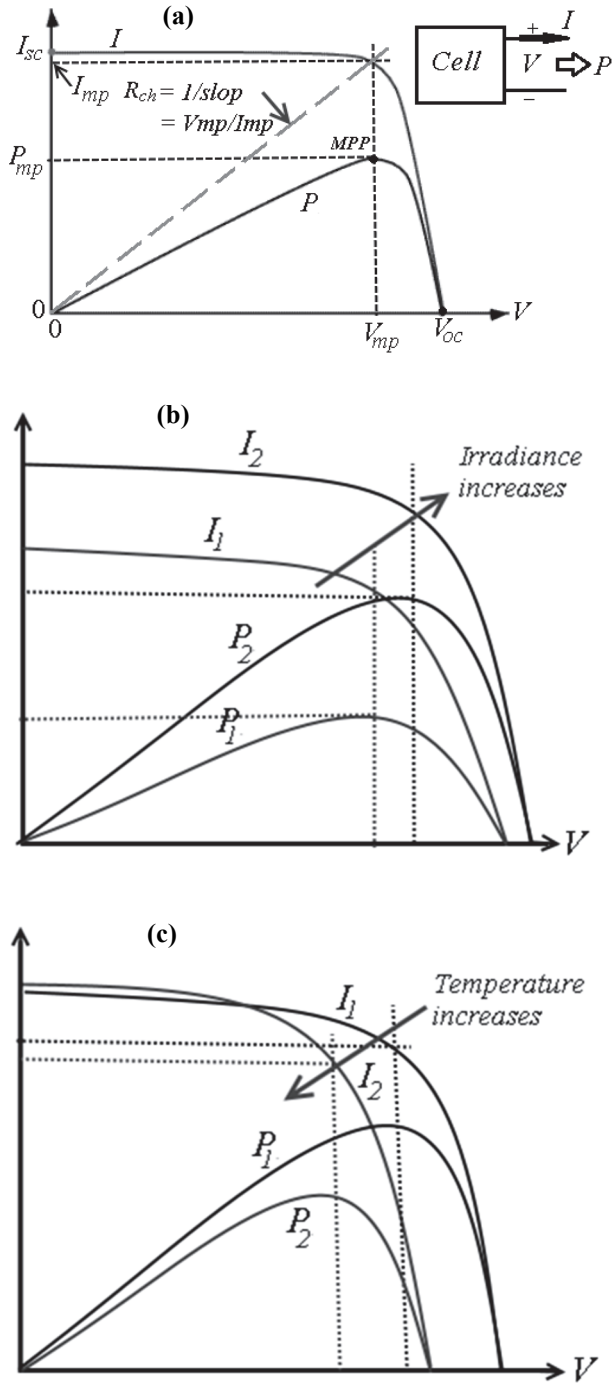

Figure 4. A typical curve characteristic of a solar-PV cell (EL-Shimy Nov 2015).
(a) I-V and P-V characteristics of a solar-PV cell;
(b) Impact of irradiance variations;
(c) Impact of temperature variations

The centrifugal pump, for example, can be characterized by its absorptive power which is obviously the mechanical power on the shaft coupled to the pump and is given by (Daud et al. 2005) $P_p = \rho\, g\, Q H_T$ and the pump efficiency is defined as the ratio of the hydraulic power imparted by the pump to the fluid to the shaft mechanical power i.e. $\eta_p = P_p / P_{mech}$. The selection of the right pump for a specific discharge rate and a definite head is usually performed via the use of the performance curves issued usually by the pump manufacturers. For a constant flow rate, the higher the pumping head the higher should be the stages number of pump and of course the associated input power. Practically, for a definite head, maximum efficiency of the centrifugal pump varies according to the flow rate in the range from 50 to 72%.

Irrigation distribution systems should have the capability to deliver and apply the amount of water needed by the crop in the appropriate time duration. The present study will focus on the most commonly used systems in Egypt which is the *flood* and *drip* irrigation distribution systems. In the surface irrigation system (*flood*), water is applied directly to the soil surface from a channel located at the upper reach of the field. Two general important requirements to obtain high efficiency in surface methods of irrigation are properly constructed water distribution systems to provide adequate control of water to the fields and proper land preparation to permit uniform distribution of water over the field (Ross et al. 1997). The micro-irrigation, also known as *trickle* or *drip* irrigation, is an irrigation method which minimizes the use of water and fertilizer by allowing water to drip slowly to the roots of plants, either onto the soil surface or directly onto the root zone. This system is used in place of water scarcity as it minimizes conventional losses like deep percolation, evaporation and run-off.

It should be noted that the main feature of *flood* irrigation is the high water discharge with low pressure on the contrary the *drip* irrigation which is featured by low discharge with a high pressure. The technique of drip irrigation in comparison with flood irrigation only wets a fraction of the soil, so that the value of the evaporation from the soil will be smaller and there will be a saving in water use. However, there will also be a greater level of transpiration as there is a greater heating of the surface (and hence of the air above it) as only a fraction of the soil is wet, so that the soil will emit more long-wave infrared irradiance. Part of this irradiance is captured by the leaves of the plant, leading to an increase in transpiration, nevertheless, the net balance of evapo-transpiration is clearly favorable to drip irrigation, especially if the plants are young and broadly space (Cuadros et al. 2004).

3. SUN TRACKING OPTIONS AND TILT ANGLE

The amount of electrical energy obtained from solar-PV systems is directly proportional to the intensity of the sunlight which falls on the solar-PV modules. For this reason it is desired that the solar-PV panels be fixed in a way that they feasibly face the sun or that they have a system which tracks the sun. The best way to collect the maximum solar energy and therefore electrical output power is by using solar tracking devices; a solar-PV systems with an appropriate sun tracking can collect 30-40% more energy than without sun tracking (Taghvaee et al. 2013).

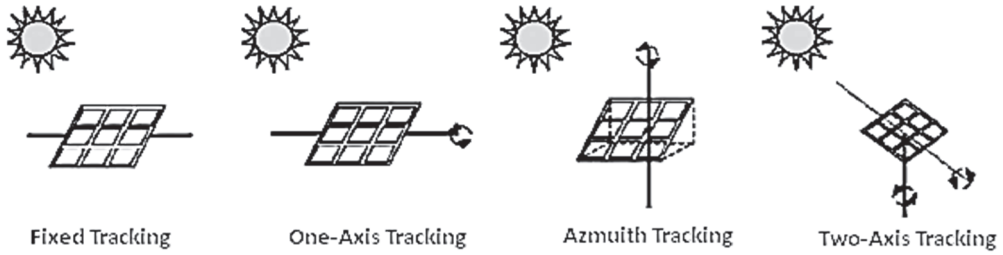

Figure 5. Types of sun tracking devices (RETScreen 2004)

A solar tracker device is a mechanical device supporting the solar collector and follows the direction of the sun on its daily sweep across the sky in a prescribed way. This is to minimize the angle of incidence of beam irradiance on the solar collector; however, the trackers are expensive, need energy for their operation and are not always can be applied. Therefore, the optimal selection of a sun tracking option is highly dependent on the coordinates of the considered site and economic feasibility of using it (Said et al. 2015). Sun tracker devices as shown in **Fig. 5** may be classified into "one-axis tracker" that track the sun by rotating around an axis located in the plane of the collector. The axis can have any orientation, but is usually horizontal east-west, horizontal north-south, or parallel to the earth's axis; "azimuth tracker" that have a fixed slope and rotate about a vertical axis; and "two-axis tracker" that always position their surface normal to the beams of the sun by rotating about two axes (RETScreen 2004).

4. SYSTEM SIZING APPROACH

The required nominal power of the solar-PV pumping system used for irrigation application is usually determined by the hydraulic energy calculation, mainly based on water demand calculated by agricultural experts, total head lift of water, monthly average daily solar irradiance values. The equation for nominal electric power of solar-PV generator or Watt peak P_{el} expressed in (W), under Standard Test Conditions (STC), according to *Kenna & Gillett* (Kenna et al. 1985)

$$P_{el} = \frac{1000}{f_m[1-\alpha_c(T_c - T_o)]\eta_{MP}} \frac{E_H}{E_S} \qquad (1)$$

where E_H is the output hydraulic energy (Wh/day), E_S is the input solar energy at the solar-PV generator (Wh/day), f_m is the load matching factor to characteristics of the solar-PV generator, α_c is the solar-PV cell temperature coefficient (°C^{-1}), T_o is the reference temperature of the cell (25 °C), η_{MP} is the motor–pump unit efficiency, and T_c is temperature of the cell (°C).

Based on **eq. (1),** the nominal electric power of solar-PV generator is calculated based on the known monthly average daily demand for hydraulic energy E_H and available monthly average daily solar irradiance E_S in the critical month (i.e. the month in which the ratio between hydraulic and radiated solar energy (E_H/E_S) is maximum) and the known efficiency of the motor-pump unit η_{MP} in reference operating conditions.

However, this approach has the following flaws:

1- The effect of solar-PV-generator tilt or tracking on its nominal capacity is absent.
2- By monitoring only the critical month, it is not possible to observe properly the demands for hydraulic energy in the other months. Furthermore, it is completely ignored that the water static level and water quantity can vary from month to month, thus affecting the determining of critical values.
3- Irrigation is considered a deferrable load because they can be supplied during any time of the day and not during specific hours. Therefore, the daily simulation of a solar-PV pumping system instead of hourly simulation would be sufficient. Subsequently, the use of the total daily irradiance in the plane of the solar-PV generator $\bar{H}_t$ instead of the monthly mean daily irradiance on the horizontal plane E_S in **Eq. (1)** will result in a better estimation of the solar energy at the input of the solar-PV generator.

In the present approach of determining the optimal nominal electric power of the solar-PV generator, **Eq. (1)** is transformed, in order to show its direct dependency on pumped water and to include characteristics of the subsystem components, as well as irrigation method. In this approach, the initial equation is the one for calculating hydraulic energy at the output of a pumping system. A pumping system demand is defined as the product of the depth from which the water is raised and the required daily flow. The daily hydraulic energy, E_H , required to pump a volume Q to a specified head H, is

$$E_H = \frac{\rho\, g\, Q\, H}{3600} \qquad (2)$$

where E_H is expressed in (W h/day),ρ is the density of water (1000 kg/m^3), g is the acceleration due to gravity (9.81 m/sec^2), Q the total daily flow of water (m^3/day) and H the total pumping head.

If the water source is a well then the total pumping head H can be expressed by (Narvarte et al. 2000),

$$H = H_{0T} + H_{ST} + \frac{H_{DT} - H_{ST}}{Q_{max}} Q_{AP} + H_F(Q_{AP}) \qquad (3)$$

where, $Q_{AP} = \sigma\, Q_d$; H is the total pumping head (m), H_{0T} is the vertical head from the water outlet to the ground (m), H_{DT} is the dynamic level of water in borehole (m),H_{ST} is

the static level (groundwater level) (m), Q_{max} is the maximum discharge capacity of well (m^3/h), Q_{AP} is the average flow rate, known as ''apparent flow''(m^3/h), H_F is the head friction loss (m), Q_d is the mean daily quantity of pumped water (m^3/day), and σ is the calculation coefficient of the average flow rate.

Furthermore, with modern solar-PV pumping systems, which are mostly electronically controlled (AC-motor-based solar-PV pumping systems), instead of matching factor f_m in **Eq. (1),** it is justified to use inverter efficiency η_I, which can include efficiency of the entire electronic system for matching the load power to the characteristics of solar-PV generator. In addition, miscellaneous solar-PV-generator losses, including solar-PV-array wiring losses, should be included. A rough estimate of these miscellaneous losses is 4% (EL-Shimy 2013; Glasnovic et al. 2007). Taking into account the losses such as: the fraction of the day in which solar irradiance is above the threshold at which the pump starts to work ($G_d > G_{thresho}$); the yield of the photovoltaic generator η_{PV} , the yield of the AC/DC inverter η_I , and the yield of the motor-pump unit η_{MP}. The hydraulic energy demand E_H is then determined according to the plant water requirements, the irrigation method, and the total pumping head:

$$E_H = \frac{\rho\, g\, Q\, H}{3600\, \eta_N \eta_F} \tag{4}$$

According to the irrigation method utilized, two efficiency factors should be included in the determination of the hydraulic energy demand. The first factor is the irrigation efficiency η_N that shows to what extent the water entering an irrigation system is exploited. The trickle (drip) irrigation method exhibits highest irrigation efficiency of 85%, while the flood irrigation method is characterized by lowest irrigation efficiency ranging from 40-50%. The irrigation efficiencies of the open-channel and sprinkle irrigation methods are 50–60% and 70%, respectively. The second factor is the efficiency of the irrigation system η_F to account for the frictional energy losses in the irrigation system. A rough estimate of these frictional energy losses is 10% (**EL-Shimy 2013**). The nominal electric power of the solar-PV generator or peak Watt P_{el} is then modified to be

$$P_{el} = \frac{\rho\, g\, Q\, H}{3600\, \bar{H}_t[1-\alpha_c(T_c - T_o)]\eta_{MP}\, \eta_N \eta_F \eta_W \eta_I} \tag{5}$$

Taking into account the power losses when the panels working at temperatures above the standard temperature 25°C. These may be taken to be approximately 10% of the nominal electric power of solar-PV generator P_{el} (Cuadros et al. 2004).The required peak solar-PV power P (kWp) will then be

$$P = 1.1 P_{el} \tag{6}$$

The actual monthly mean produced energy available for water pumping in (KWh/day) E_A is given by (EL-Shimy 2013):

$$E_A = A\, \eta_{MP}\, \eta_r\, \eta_W \eta_I \bar{H}_t[1-\alpha_c(T_{cell} - T_o)] \tag{7}$$

where, A is the overall area of the solar-PV generator given by ($A = m * s$), s is the area of solar-PV module, η_r is the solar-PV module efficiency at a reference temperature, and η_W is the miscellaneous solar-PV-array losses (wiring losses). The number of solar-PV modules m is defined by ($m = P^*_{el}/P_{Module}$) which should be approximated to the nearest highest integer number and P^*_{el} is the optimal nominal electric power of the solar-PV generator.

The actual pumped total daily water flow Q_{pumped} in (m^3/day) can be determined by:

$$Q_{pumped} = \frac{3600\, E_A\, \eta_N \eta_F}{\rho\, g\, H} \tag{8}$$

The overall efficiency of the solar-PV water pumping system can be determined by:

$$\eta_A = \eta_{MP}\, \eta_N \eta_F \eta_W \eta_I \eta_r [1-\alpha_c(T_{cell} - T_o)] \tag{9}$$

Although the given sizing model seems simple, it is not easy to size the solar-PV pumping system to produce the expected hydraulic energy in every time stage, because the produced hydraulic energy from solar-PV pumping system depends on radiated solar energy in that period. Due to this, this work defines the objective function in a new way, i.e., by optimizing the relation between the output hydraulic energy and the input produced energy. The minimization of the objective function in this work results in finding the nominal electric power of the solar-PV generator which would, in the observed period, meet the consumers' demands in the best way possible. This will be described in the upcoming sections of this paper.

5. LEVELIZED COST OF ENERGY (LCOE)

It should be noted that, an economic feasibility study conducted for a certain location at particular time may not be applicable for another location and at another time. Generally, the economic feasibility of an energy production project can be evaluated using several metrics (EL-Shimy 2013; El-Shimy 2012; Branker et al. 2011). One of these metrics is the cost per watt, but this method does not consider the effects of the lifetime, performance of the energy producing equipment, and the financial policies. The levelized cost of energy (LCOE) is another popular metric which is a cost of producing energy (usually electricity) for a particular system. Therefore, it fairly compares the energy costs produced by different systems, and it allows alternative technologies to be compared when different scales of operation, investment or operating time periods exist. The LCOE is the net present value of the unit-cost of electricity over the lifetime of a generating technology. It is often taken as a representation for the average price that the generating technology must receive in a market to break even over its lifetime. The LCOE captures capital costs, ongoing system-related costs and fuel costs- along with the amount of electricity produced- and converts them into a common metric: $/kWh.

Details about the mathematical modeling of the LCOE is available in (Said et al. 2015); however, generally, the LCOE can be defined by

$$LCOE = \frac{Total\ Life\ Cycle\ Cost\ (TLCC)}{Total\ Lifetime\ Energy\ Production} \quad (10)$$

6. THE TRUE COST OF ELECTRICITY GENERATION TECHNOLOGIES

In the energy markets across the world, market prices for fossil fuels are often lower than the prices of energy generated from renewable sources, such as solar, and wind. These market prices, however, don't consider the "true costs" of the energy being sold, because they ignore the external costs to society caused by pollution and its resulting problems, including damages to public health and the environment (Burtraw et al. 2012). **Table 1** illustrates that this metric ignores the huge variation in external cost estimates due to their sensitivity to the presence of multidimensional components of external damages. Median values might be a better indication of central tendency than mean values because they do not allow outliers to influence the measure.

7. GREEN HOUSE GASES (GHG) ANALYSIS

Among the available software for analysis of renewable energy technologies, the powerful freeware *RETScreen* Clean Energy Project Analysis version 4.0 software is used in this study to perform the Green House Gases (GHG) emission reduction analysis. The RETScreen software is capable of estimating the amount of greenhouse gases (GHG) which could be avoided as a result of usage of renewable energy sources. It determines the greenhouse gas emission reduction (mitigation) potential for a Base Case System (Baseline), and for the Proposed Case System (Clean Energy Project).This GHG emission reduction analysis worksheet contains four main sections: Background Information, Base Case System (Baseline), Proposed Case System (Project) and GHG Emission Reduction Summary. The results are calculated as equivalent tonnes of CO_2 avoided per annum (El-Shimy 2009; RETScreen 2004).

The model indicates the global warming potential (GWP) of methane (CH_4) and nitrous oxide (N_2O). GWPs have been assigned to greenhouse gases to allow for comparisons of their relative heat-trapping effect. The higher the GWP of a gas the greater the contribution to the greenhouse effect (RETScreen 2004). GWPs of gases are describes the influence of a GHG in comparison to carbon dioxide (CO_2), which is assigned a GWP of 1, (i.e., the GWP of CH_4 is 21 means that a ton of methane is considered to cause 21 times more global warming than a ton of carbon dioxide and the GWP of N_2O is 310 means that a ton of nitrous oxide is considered to cause 310 times more global warming than a ton of carbon dioxide). The default values are defined by International Panel on Climate Change (IPCC) (Sundqvist et al. 2002).

In the present work, the engine driven pump with diesel as the fuel type and grid extension with oil as the fuel type were selected as the baseline cases. The default emission factors (i.e. the mass of greenhouse gas emitted per unit of energy and vary for different types and qualities of fuels, and for different types and sizes of power plants) and conversion efficiencies (i.e. the efficiency of energy conversion from primary heat potential to actual useful energy output) of diesel and oil fuel types are given in **Table 2** (Fenhann 1999).

Table 1. Summary of External Cost Estimates from the Literature (Burtraw et al. 2012)

Cents/kWh	Coal	Oil	Natural Gas	Nuclear	Hydro	Wind	Solar	Biomass
Min	0.01	0.04	<0.01	<0.01	0	0	0	0
Max.	90.61	53.43	17.69	86.23	35.14	1.18	2.94	29.56
Mean	18.75	16.48	6.17	9.53	4.50	0.41	1.12	6.62
Median	8.54	12.19	3.51	1.08	0.43	0.43	1.02	3.59

Table 2. Default emission factors and conversion efficiency of various fuels (Fenhann 1999)

Fuel type/ Source	CO_2 emission factor e_{co_2} (Kg/Gj)	CH_4 emission factor e_{CH_4} (Kg/Gj)	N_2O emission factor e_{N_2O} (Kg/Gj)	Fuel conversion efficiency η (%)
Diesel	74.10	0.0020	0.0020	30
Oil	77.40	0.0030	0.0020	30
solar-PV	00.00	0.0000	0.0000	43

In the RETScreen software, in case of the "Grid extension" is the baseline power source, it is often reasonable to assume that an oil fired power plant is the proxy plant, with "oil" is the fuel type with a 100% fuel mix and the default Transmission and Distribution "T & D" losses is 15% which includes all energy losses between the power plant and the end-user. In addition, for "Water pumping" (where the fuel conversion efficiency equals the solar-PV pump system efficiency) is assumed to be 43% (RETScreen 2004).

8. METHODOLOGY

A flowchart for the sizing evaluation is given in **Fig. 6.** Extensive analysis of the meteorological conditions of the study site is performed to ensure the compatibility of the site's characteristics with the Standard Operating Conditions (SOC) required by the all the solar-PV modules listed in RETScreen software database. An appropriate solar correlation model for the specific site is determined. To ensure the capability of the generated energy, the sizing

decision is based on the simulation of the solar-PV pumping system over the whole year. The optimal sizing is evaluated by comparing the monthly average hydraulic energy demand and the actual monthly average produced energy available for water pumping.

An optimally sized solar-PV pumping system will be able to supply the required hydraulic energy for all the months of the year. Therefore, the optimal capacity of an optimally tilted solar-PV generator P_{el}^{*} is determined by the following equation:

$$P_{el}^{*} = \max\left(P_{el}(i)\right), \tag{11}$$

where, $i = 1, 2, 3, \ldots\ldots, 12$ is the number of the month such that i = 1 for January and i = 12 for December.

The governing constraints that, if satisfied, indicate an optimally sized solar-PV water pumping system are:

$$\left.\begin{array}{c} E_A(i) - E_H(i) \geq 0 \\ \max\left(E_A(i)\right) - \max\left(E_H(i)\right) \cong 0 \end{array}\right\} \tag{12}$$

These constraints can be used to evaluate the optimal sizing of the solar-PV. In **eq. 12**, the first constraint is an inequality constraint, which is included to ensure the sufficiency of the solar-PV generator to supply the demanded monthly mean hydraulic energy for all months. The satisfaction of the second constraint prevents over-sizing of the solar-PV generator (EL-Shimy 2013). In order to conduct an economic feasibility analysis for renewable energy projects, initial costs, periodic costs, and financial parameters are required as inputs. Since, it is internationally agreed that large value of uncertainty are associated with these parameters; however, the input economical parameters used in this paper are obtained from literature such as energy cost escalation rate, interest rate, inflation rate, discount rate, etc are summarized in **Table 3.**

Table 3. Summary of various financial parameters used in this study

Item description	Value
Inflation rate	10.96%
Real discount rate	9.25%
Annual debt interest rate	8.75%

The subsidies and incentives for solar-PV systems include tax rebates, grants, feed-in tariffs, net metering and Renewable Energy Certificates (RECs). Since subsidies and incentives are complex and widely variant, they are not considered in the present study. Income taxes and credits are not considered in this study. The omission of these economic items will also result in safe viability analysis results and conclusions.

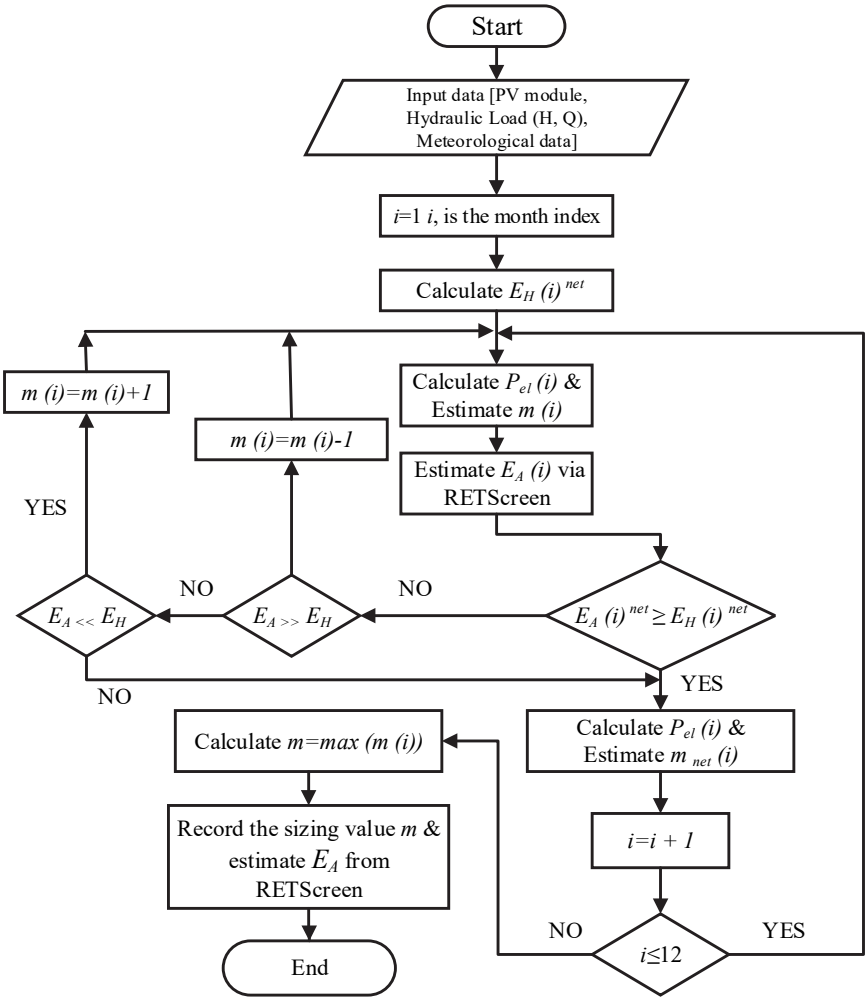

Figure 6. A flowchart for the sizing evaluation.

Table 4. Electricity tariff prices for agriculture sector in Egypt.

Fiscal year	2008/2009	2014/2015	2015/2016	2016/2017	2017/2018	2018/2019
Tariff PT/kWh	11.20	17.00	22.00	27.10	33.40	41.10
Escalation rate %	N/A	51.79	29.41	23.18	23.25	23.05

In order to calculate the power rating for the appropriate engine to drive the pump, P_{Engine} the following equation can be used

$$P_{Engine} = \frac{P_P}{F} \tag{13}$$

where F is the load factor of the engine which will be assumed by 80 % and P_P is the power required by the pump/motor which can determined by (Muselli et al. 1999)

$$P_P = \frac{\rho\ g\ h\ Q}{\eta_{mp}} \tag{14}$$

where Q is the maximum volumetric flow rate in m^3/sec, ρ is the density of water in Kg/m^3, g is the gravitational constant in m/sec^2, h is the total dynamic head in meters, and η_{mp} is the pump/motor efficiency which is assumed to be 43%.

The capital cost of the diesel engine is then estimated using,

$$C_{Engine} = \$234.23\ P_{Engine} + \$3400 \tag{15}$$

Eq. (15) is based on generator dealer pricing (Brighton CO 2016; Caterpillar Inventory 2016). Prices are assumed to include the cost of the associated control electronics. An installation cost of 10% of the retail price is assumed. The total capital cost of the diesel generator system, C_{Engine} is then given by,

$$C_{Total} = 1.1\ C_{Engine} \tag{16}$$

In order to calculate the required diesel fuel consumption, the Specific Fuel Consumption (SFC) should be estimated. The SFC includes the efficiency of both the source and pump, expressed in L_{Fuel}/L_{Water}, it allows specifying the value of fuel liters needed per liter of pumped water. The SFC can be estimated by the following equation (RETScreen 2004),

$$SFC = \frac{9.81 \times H}{J \times \eta_{engine} \times \eta_{pump}} \tag{17}$$

where, H is the total head (m), J is the energy content of fuel (38.7 MJ/L), η_{engine} is the engine efficiency = 80% and η_{pump} is the pump efficiency which is assumed to be 65%.

The diesel engine poses additional running costs resulting from the intensive operation, monitoring and maintenance requirements. The diesel system contains air, fuel, oil, and water separator filters that require replacement. Lubrication oil and coolant need to be replaced periodically. Therefore, a diesel engine should be continuously a subject for intensive monitoring and maintenance. Frequent damages for diesel engine occur. Consequently, a considerable stock of spare parts should be available on-site. Additionally, oil should be changed every 250 operating hours and a complete overhaul should be conducted every 15,000 operating hours (Muselli et al. 1999). The annual O&M costs of a diesel engine are considered to have about 15% of the capital costs and the lifetime of the engine is assumed to be 13 years (Qoaider et al. 2010).

The utility electricity prices differ according to the consumer class (i.e. residential, commercial, industrial and agriculture etc.) and the voltage level of the power supply (i.e. low voltage, medium voltage, high voltage etc.). Each class or voltage level has its own price. In Egypt, a tiered retail electricity-pricing scheme is used. The tariff is converted to (US$ cents/kWh). In 2008, the electricity tariff for agriculture application, that is connected mainly to the low voltage network 380 V, was 11.2 PT/kWh which increased to 17 PT/kWh in July 2014 according to the cabinet decree No. 1257 year 2014, which decided that the electricity tariff will be increased gradually over the next five years starting from the fiscal year 2014 to 2018 in a move to liberate the electricity market as it is still subsidized as shown in **Table 4** (EgyptERA 2016).

For this analysis proposed here, price escalation rate after Fiscal year 2018/2019 is assumed to be 23 % per year.

The meteorological conditions and the proposed hydraulic energy demand are available in (EL-Shimy 2013). **Fig. 7** compares the demanded hydraulic energy in case of a flood and drip irrigation system. It should be mentioned that the used irrigation efficiency for flood and drip systems which is necessary to calculate the hydraulic energy demand is 45% and 85% respectively.

The highest hydraulic energy demand, as shown in **Fig. 7**, occurs in June, July and August months, independent of the irrigation methods, like the daily solar irradiance on a horizontal surface at which the highest irradiances are in June, July and August months (summer months), this reveals that the highest irrigation water demand that occurs in summer months meet the highest solar irradiances which make the solar-PV powered water pumping is an excellent choice. The demanded hydraulic energy values in case of drip irrigation system is lower than those values in case of flood system with about 52.94 % for all the months. This indicates that the drip irrigation system is an energy saving system rather than the flood one.

9. RESULTS

9.1 Optimal tilt angle

For determining the optimal sun tracking type and the optimal tilt angle, two stages are performed. In the *first*

stage, the optimal tracking type (fixed, one-axis, and two-axis) is determined by comparing the output energy with various tracking options and the optimal option is selected based on the highest output energy. In the *second stage*, the optimal time based tilt angle (annual, monthly, and seasonally) is determined by comparing the output energy for the different solar-PV technologies for the optimal sun tracking type. **Tables 5-7** summarize the comparison of the output energy of the different tracking types in case of annual, monthly, and seasonally time based respectively. The tables also show the values of the energy production from the modules considering two situations. The first one is horizontally placed solar-PV module $\beta = 0$, while the second situation is module with the optimal theoretical tilt angle (which is $\beta = \psi - \delta$= 23.33°) where ψ is the latitude of the site and δ is the declination angle.

It is clear from **Table 5** that, for any solar-PV technology, the output energy of the estimated and theoretical annual fixed angle and annual one-axis is the same. The output energy of the annual two-axis tracking type is higher than the estimated and theoretical annual one-axis by a value does not exceed 4% (2.96%, 3.04%, 3.16%, 3.85%, 2.99% for mono-Si, Poly-Si, a-Si, CdTe, CIS respectively) and higher than and the annual fixed type by a value exceeding 35% (35.88%, 36.10%, 36.11%, 35.97%, 36.18% for mono-Si, Poly-Si, a-Si, CdTe, CIS respectively). In addition, the output energy of the estimated and theoretical annual one-axis is higher than the estimated and theoretical annual fixed tracking type by a value exceeding 30% (31.97%, 32.09%, 31.94%, 30.94%, 32.24% for mono-Si, Poly-Si, a-Si, CdTe, and CIS respectively). Taking into consideration the high cost of the two-axis tracking type and the small output energy difference with the one-axis tracking type, it should be concluded that the annual one-axis is the optimal tracking type.

Table 5. The output energy for different solar-PV modules and for annual based tracking types (MWh/y).

Tracking type		Annual Fixed			Annual One-Axis			Annual Two-Axis
Tilt angle		Estimated (20.4°)	Horizontal (0°)	Theoretical (23.33°)	Estimated (22°)	Horizontal (0°)	Theoretical (23.33°)	
solar-PV tech	Mono-Si	0.588	0.563	0.588	0.776	0.755	0.776	0.799
	poly-Si	0.349	0.334	0.349	0.461	0.448	0.461	0.475
	a-Si	0.288	0.275	0.288	0.380	0.369	0.380	0.392
	CdTe	0.139	0.133	0.139	0.183	0.178	0.182	0.189
	CIS	0.152	0.146	0.152	0.201	0.196	0.201	0.207

Table 6. The output energy for different solar-PV modules and for monthly based tracking types (MWh/y).

Tracking type		Monthly Fixed			Monthly One-Axis			Monthly Two-Axis
Tilt angle		Estimated	Horizontal (0°)	Theoretical	Estimated	Horizontal (0°)	Theoretical	
solar-PV tech	mono-Si	0.621	0.563	0.617	0.794	0.755	0.794	0.799
	poly-Si	0.367	0.335	0.367	0.472	0.447	0.471	0.475
	a-Si	0.303	0.274	0.302	0.391	0.369	0.390	0.392
	CdTe	0.147	0.134	0.146	0.188	0.176	0.186	0.189
	CIS	0.159	0.146	0.160	0.206	0.197	0.206	0.207

Table 7. The output energy for different solar-PV modules and for seasonally based tracking types (MWh/y)

Tracking type		Seasonally Fixed			Seasonally One-Axis			Seasonally Two-Axis
Tilt angle		Estimated	Horizontal (0°)	Theoretical	Estimated	Horizontal (0°)	Theoreti-cal	
solar-PV tech	mono-Si	0.614	0.563	0.612	0.792	0.755	0.791	0.799
	poly-Si	0.366	0.335	0.365	0.470	0.447	0.469	0.475
	a-Si	0.300	0.275	0.300	0.388	0.367	0.388	0.392
	CdTe	0.144	0.132	0.144	0.187	0.176	0.186	0.189
	CIS	0.159	0.146	0.158	0.206	0.197	0.205	0.207

Table 8. The output energy for different solar-PV technology for the time based one-axis tracking type

Output Energy (MWh/y) for one-axis tracking type				
Time segment		Annual	Monthly	Seasonally
solar-PV tech	mono-Si	0.776	0.794	0.792
	poly-Si	0.461	0.472	0.470
	a-Si	0.380	0.391	0.388
	CdTe	0.183	0.188	0.187
	CIS	0.201	0.206	0.206

It is clear from **Table 6** that, for any solar-PV technology the output energy of the estimated and theoretical monthly fixed angle and monthly one-axis is almost the same. The output energy of the monthly two-axis tracking type is higher than the estimated and theoretical monthly one-axis by a value does not exceed 1% (0.63%, 0.64%, 0.26%, 0.53%, 0.49% for mono-Si, Poly-Si, a-Si, CdTe, CIS respectively) and higher than the estimated and theoretical monthly fixed type by a value exceeding 28% (28.66%, 29.43%, 29.37%, 28.57%, 30.19% for mono-Si, Poly-Si, a-Si, CdTe, CIS respectively). The output energy of the estimated and theoretical monthly one-axis is higher than the estimated and theoretical monthly fixed tracking type by a value exceeding 27% (27.86%, 28.61%, 29.04%, 27.89%, 29.56% for mono-Si, Poly-Si, a-Si, CdTe, and CIS respectively). Taking into consideration the high cost of the two-axis tracking type and the small output energy difference with the one-axis tracking type, it should be concluded that the monthly one-axis is the optimal tracking type.

It is clear from **Table 7** that, for any solar-PV technology the output energy of the estimated and theoretical seasonally fixed angle and seasonally one-axis is almost the same. The output energy of the seasonally two-axis tracking type is higher than the estimated and theoretical seasonally one-axis by a value does not exceed 1% (0.88%, 1.06%, 1.03%, 1.07%, 0.49% for mono-Si, Poly-Si, a-Si, CdTe, CIS respectively) and higher than the seasonally fixed by a value exceeding 29% (30.13%,29.78%, 30.67%, 31.25%, 30.19% for mono-Si, Poly-Si, a-Si, CdTe, CIS respectively). In addition, the output energy of the estimated and theoretical seasonally one-axis is higher than the estimated and theoretical seasonally fixed type by a value exceeding 28% (28.99%, 28.42%, 29.33%, 29.86%, 29.56% for mono-Si, Poly-Si, a-Si, CdTe, and CIS respectively). Taking into consideration the high cost of the two-axis tracking type and the small output energy difference with the one-axis tracking type, it should be concluded that the seasonally one-axis is the optimal tracking type. In the *Second Stage*, the time based tilt angle (Annual, Monthly, Seasonally) is determined by comparing the output energy for the different solar-PV technologies for the determined optimal tracking type. Table 8 shows the output energy based on the estimated tilt angle only for the optimal tracking type (one-axis) as it is slightly higher than in case of the theoretical angle.

It is depicted from **Table 8** that the output energy in case of the monthly based tilt angle is higher than in case of seasonally based tilt angle by 0.25%, 0.43%, 0.77%, 0.53, 0% for mono-Si, Poly-Si, a-Si, CdTe, CIS solar-PV modules respectively. While the output energy in case of the seasonally based tilt angle is higher than the annual based tilt angle by 2.06%, 1.95%, 2.11%, 2.19%, 2.40% for mono-Si, Poly-Si, a-Si, CdTe, CIS modules respectively. Therefore the seasonally based tilt angle for the one-axis tracking type is the optimum choice.

9.2. Optimal sizing of the solar-PV generator

Tables 9 - 12 show the results based on the seasonally based tilt angle for the one-axis tracking type as chosen the optimum choice.

Table 9: The number of solar-PV module (m) of the solar-PV generator

Sizing Parameter			$Number\ of\ modules - m$; seasonal one-axis tracking									
solar-PV Type & Model			mono-Si-SPR 320E-WHT		poly-Si-CS6A 190W		a-Si- SN2-145.0W		CdTe- AB1-72		CIS- SL1-85W	
Irrigation method			Flood	Drip	Flood	Drip	Flood	Drip	Flood	Drip	Flood	Drip
Winter			35,393	18,739	59,609	31,560	73,479	38,904	151,364	80,140	136,316	72,172
Jan	Feb	Mar										
Spring			44,871	23,748	75,572	39,996	89,422	47,338	187,531	99,249	174,662	92,438
Apr	May	Jun										
Summer			48,503	25,688	81,689	43,264	96,719	51,225	202,763	107,388	188,706	99,943
Jul	Aug	Sep										
Autumn			35,893	18,995	60,451	31,990	75,658	40,038	154,791	81,914	137,666	72,852
Oct	Nov	Dec										

Table 10: The total collector area (S) of solar-PV generator

Sizing Parameter			$Overall\ area - S\ (m^2)$; seasonal one-axis tracking									
solar-PV Type & Model			mono-Si-SPR 320E-WHT		poly-Si-CS6A 190W		a-Si- SN2-145.0W		CdTe- AB1-72		CIS- SL1-85W	
Irrigation method			Flood	Drip	Flood	Drip	Flood	Drip	Flood	Drip	Flood	Drip
Winter			57,337	30,357	77,492	41,028	130,793	69,249	108,983	57,701	102,237	54,129
Jan	Feb	Mar										
Spring			72,691	38,472	98,244	51,995	159,171	84,262	135,02	71,459	130,997	69,326
Apr	May	Jun										
Summer			78,575	41,615	106,196	56,243	172,160	91,180.5	108,982	57,701	141,530	74,957
Jul	Aug	Sep										
Autumn			58,147	30,772	78,586	41,587	134,671	71,268	135,022	71,459	103,250	54,639
Oct	Nov	Dec										

Table 11: The nominal electric power(P_{el}) of the solar-PV generator

Sizing Parameter			P_{el} (MWp); seasonal one-axis tracking									
solar-PV Type & Model			mono-Si-SPR 320E-WHT		poly-Si-CS6A 190W		a-Si- SN2-145.0W		CdTe- AB1-72		CIS- SL1-85W	
Irrigation method			Flood	Drip	Flood	Drip	Flood	Drip	Flood	Drip	Flood	Drip
Winter			11.33	6.00	11.33	6.00	10.65	5.64	10.90	5.77	11.59	6.13
Jan	Feb	Mar										
Spring			14.36	7.60	14.36	7.60	12.97	6.86	13.50	7.15	14.85	7.86
Apr	May	Jun										
Summer			15.52	8.22	15.52	8.22	10.65	5.64	14.60	7.73	16.04	8.50
Jul	Aug	Sep										
Autumn			11.49	6.08	11.49	6.08	12.97	6.86	11.14	5.90	11.70	6.19
Oct	Nov	Dec										

Table 12: The monthly mean available produced energy(E_A) of the solar-PV generator

Sizing Parameter			E_A (MWh/month); seasonal one-axis tracking									
solar-PV Type & Model			mono-Si-SPR 320E-WHT		poly-Si-CS6A-190W		a-Si- SN2-145.0W		CdTe- AB1-72		CIS- SL1-85W	
Irrigation method			Flood	Drip	Flood	Drip	Flood	Drip	Flood	Drip	Flood	Drip
Winter			8,657	4,585	8,657	4,585	8,199	4,343	8,397	4,447	8,780	4,651
Jan	Feb	Mar										
Spring			10,678	5,655	10,678	5,655	10,578	5,602	10,621	5,625	10,702	5,668
Apr	May	Jun										
Summer			10,262	5,435	10,262	5,435	10,254	5,431	10,257	5,433	10,262	5,436
Jul	Aug	Sep										
Autumn			7,752	4,106	7,752	4,106	7,430	3,935	7,570	4,009	7,846	4,155
Oct	Nov	Dec										

It is clear from **Tables 9 - 12**, for the one-axis seasonally based tracking type, the used number of solar-PV modules and its collector area in case of drip irrigation method is lower than the flood irrigation case by almost 47.06 % for all solar-PV technologies. It is also clear that the P_{el} of solar-PV modules in case of drip irrigation method is lower than the flood irrigation caseby almost 47.06 %. On the same manner, the E_A at the maximum number of solar-PV modules in case of drip irrigation method is lower than the flood irrigation case by almost 47.04 %.

The results also show that the minimum number of the required modules and the minimum collector area is associated with the mono-Si technology considering the mono-Si-SPR 320E-WHT module. On the other hand, the minimum nominal electric power is associated with the thin film technology of the a-Si- SN2-145.0W modules while the maximum available energy is associated with the thin film technology of the CIS- SL1-85W modules. Therefore, the crystalline solar-PV technologies offer low collector area in comparison with the thin film technologies but the thin film technologies offer higher energy. In this paper, the maximization of the land use saving is assumed to be significantly important. Therefore, the mono-Si-SPR 320E-WHT modules are considered in the construction of the solar-PV generator and the subsequent analysis.

9.3. LCOE results

Considering the true cost of energy, the LCOE is estimated for various energy alternatives i.e. solar-PV, diesel engine, and grid electricity. It is found that the LCOE of solar-PV driven pump is 0.071, 0.070, 0.069 and 0.067 ($/KWh) for debt ratios (DR) of 100%, 75%, 50% and 0% respectively. It is also found that the LCOE of Engine driven pump is 0.220, 0.217, 0.215 and 0.210 ($/kWh) for DR of 100%, 75%, 50% and 0% respectively. The LCOE of grid electricity driven pump is found to be 0.193 ($/kWh). The results show that the solar-PV is the most economical energy source followed by the grid electricity then the diesel engine.

9.4. Green House Gases (GHG) analysis

Fig. 8 shows the GHG analysis results. As expected, the results show that the solar-PV generator is the most environmental friendly energy alternative followed by the diesel engine then the grid electricity.

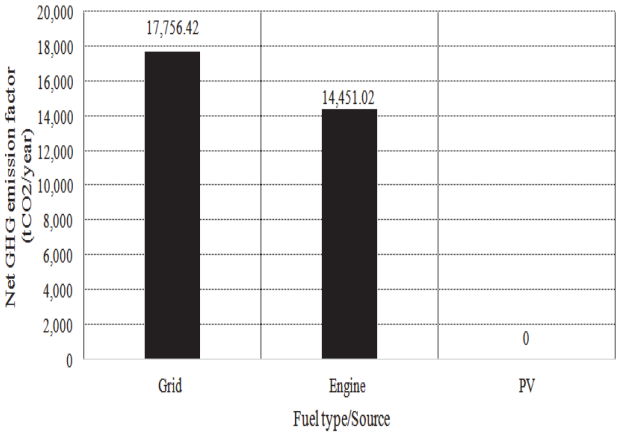

Fig. 8: Net GHG emission factors for various energy alternatives

10. CONCLUSIONS

This paper presented an improved modeling and viability analysis for optimal sizing and performance analysis of solar-PV sources for irrigation water pumping (IWP) systems considering various solar-PV technologies as well as various sun tracking options. Other traditional alternatives for powering IWP systems are considered and compared with the solar-PV alternative. The considered traditional sources are the diesel engines and the utility grid electricity.

The results show that the one-axis sun tracking is the most feasible alternatives as it provides an energy production gain comparable with the two-axis tracking while its cost is relatively low in comparison with the two-axis tracking. The energy production gain with the seasonally tilted one-axis tracking is significantly high in comparison with the fixed modules. From solar-PV technological points of view, the results show that the optimally selected crystalline solar-PV technologies offer low collector area in comparison with the thin film technologies but the thin film technologies offer higher energy production. From economical point of view, the LCOE estimations show that the solar-PV is the most economical energy source followed by the grid electricity then the diesel engine. In addition, the GHG analysis shows that the solar-PV generator is the most environmental friendly energy alternative followed by the diesel engine then the grid electricity.

12. REFERENCES

Bachus L, Custodio A. Know and Understand Centrifugal Pumps: Elsevier Science; 2003.

Branker K, Pathak M, Pearce JM. A review of solar photovoltaic levelized cost of electricity. Renewable and sustainable energy reviews. 2011;15(9):4470-82.

Brighton CO. [cited 2016 June 1, 2016]; Available from: http://www.dieselserviceandsupply.com/New-Generators/.

Burtraw D, Krupnick A, Sampson G, Beasley B. The true cost of electric power. RFF Report, Resources for the Future, Washington, DC[online][cit 0111 2013] Available at: http://www rff org/RFF/Documents/RFF-Rpt-BurtrawKrupnick% 20TrueCosts pdf. 2012.

Caterpillar Inventory. Express generators power suppliers. 2016; Available from: http://www.expressgenerators.com/inventory.html.

Cloutier M, Rowley P. The feasibility of renewable energy sources for pumping clean water in sub-Saharan Africa: A case study for Central Nigeria. Renewable Energy. 2011;36(8):2220-6.

Cuadros F, López-Rodrıguez F, Marcos A, Coello J. A procedure to size solar-powered irrigation (photoirrigation) schemes. Solar energy. 2004;76(4):465-73.

Daud A-K, Mahmoud MM. Solar powered induction motor-driven water pump operating on a desert well, simulation and field tests. Renewable Energy. 2005;30(5):701-14.

De Brito MA, Sampaio LP, Luigi G, e Melo GA, Canesin CA. Comparative analysis of MPPT techniques for PV applications. Clean Electrical Power (ICCEP), 2011 International Conference on: IEEE; 2011. p. 99-104.

Duffie JA, Beckman WA. Solar Engineering of Thermal Processes: Wiley; 2013.

Duzat M, Siqueira RMd. Analytical and experimental investigation of photovoltaic pumping systems: Universität Oldenburg; 2000.

EgyptERA. Electricty Tariffs, Egypt 2014. Cairo: Egyptian Electric Utility and Consumer Protection Regulatory Agency EgyptERA; 2016; Available from: http://egyptera.org/en/t3reefa.aspx.

El-Shimy M. Viability analysis of PV power plants in Egypt. Renewable Energy. 2009;34(10):2187-96.

El-Shimy M. Analysis of Levelized Cost of Energy (LCOE) and grid parity for utility-scale photovoltaic generation systems. 15th International Middle East Power Systems Conference (MEPCON'12); Dec. 23-25, 2012; Cairo, Egypt: IEEE; 2012. p. 1-7.

El-Shimy M. Sizing optimisation of stand-alone photovoltaic generators for irrigation water pumping systems. International Journal of Sustainable Energy. 2013;32(5):333-50.

EL-Shimy M. Dynamic Security of Interconnected Electric Power Systems: Omniscriptum Gmbh & Company Kg.; May, 2015.

EL-Shimy M. Dynamic Security of Interconnected Electric Power Systems - Volume 2: Dynamics and Stability of Conventional and Renewable Energy Systems: LAP Lambert Academic Publishing; Nov, 2015.

EL-Shimy M, Abdo T. PV Technologies: History, Technological Advances, and Characterization. In: Anwar S, editor. Encyclopedia of Energy Engineering and Technology Taylor & Francis - CRC Press; 2015.

EL-Shimy M, Durin B. Techno-Economic Evaluation and Sizing Optimization of Solar-PV and Wind Energy Sources for Irrigation Water Pumping. The international congress of energy and environment 2016; Opatija, Croatia2016.

Faranda R, Leva S. A Comparative Study of MPPT techniques for PV Systems. 7th WSEAS International Conference on Application of Electrical Engineering (AEE'08); Trondheim, Norway2008. p. 100-5.

Fenhann JV. Projections of emissions of greenhouse gases, ozone precursors and sulphur dioxide from Danish sources until 2012: Energistyrelsen; 1999.

Ghoneim A. Design optimization of photovoltaic powered water pumping systems. Energy conversion and management. 2006;47(11):1449-63.

Glasnovic Z, Margeta J. A model for optimal sizing of photovoltaic irrigation water pumping systems. Solar energy. 2007;81(7):904-16.

Gopal C, Mohanraj M, Chandramohan P, Chandrasekar P. Renewable energy source water pumping systems—A literature review. Renewable and sustainable energy reviews. 2013;25:351-70.

Hamidat A, Benyoucef B. Mathematic models of photovoltaic motor-pump systems. Renewable Energy. 2008;33(5):933-42.

Hamidat A, Benyoucef B, Hartani T. Small-scale irrigation with photovoltaic water pumping system in Sahara regions. Renewable Energy. 2003;28(7):1081-96.

Kenna J, Gillett WB. Solar Water Pumping: A Handbook: Intermediate Technology Publications; 1985.

Lal S, Kumar P, Rajora R. Techno-economic analysis of solar photovoltaic based submersible water pumping system for rural areas of an Indian state Rajasthan. Science Journal of Energy Engineering. 2013;1(1):1-4.

Muselli M, Notton G, Louche A. Design of hybrid-photovoltaic power generator, with optimization of energy management. Solar energy. 1999;65(3):143-57.

Muselli M, Notton G, Louche A. Design of hybrid-photovoltaic power generator, with optimization of energy management. Solar energy. 1999;65(3):143-57.

Narvarte L, Lorenzo E, Caamaño E. PV pumping analytical design and characteristics of boreholes. Solar energy. 2000;68(1):49-56.

NASA. Surface meteorology and Solar Energy. USA: NASA; 2016 [cited 2016 10/5/2016]; Available from: http://www.eosweb.larc.nasa.gov/sse/.

Pande P, Singh A, Ansari S, Vyas S, Dave B. Design development and testing of a solar PV pump based drip system for orchards. Renewable Energy. 2003;28(3):385-96.

Qoaider L, Steinbrecht D. Photovoltaic systems: a cost competitive option to supply energy to off-grid agricultural communities in arid regions. Applied Energy. 2010;87(2):427-35.

Ramos J, Ramos HM. Solar powered pumps to supply water for rural or isolated zones: a case study. Energy for Sustainable Development. 2009;13(3):151-8.

RETScreen International. Clean Energy Decision Support Centre. Clean Energy Project Analysis: RETScreen Engineering & Cases Textbook : Photovoltaic Project Analysis Chapter: Minister of Natural Resources Canada; 2004.

Ross E, Hardy L. National Engineering Handbook: Irrigation guide: U.S. Department of Agriculture, Natural Resources Conservation Service; 1997.

Said M, EL-Shimy M, Abdelraheem M. Photovoltaics energy: Improved modeling and analysis of the levelized cost of energy (LCOE) and grid parity–Egypt case study. Sustainable Energy Technologies and Assessments. 2015;9:37-48.

Sundqvist T, Söderholm P. Valuing the environmental impacts of electricity generation: a critical survey. The Journal of Energy Literature. 2002.

Taghvaee M, Radzi M, Moosavain S, Hizam H, Marhaban MH. A current and future study on non-isolated DC–DC converters for photovoltaic applications. Renewable and sustainable energy reviews. 2013;17:216-27.